Multiseriate cortical sclerenchyma enhance root penetration in compacted soils

Hannah M. Schneider[a], Christopher F. Strock[a], Meredith T. Hanlon[a], Dorien J. Vanhees[b,c], Alden C. Perkins[a], Ishan B. Ajmera[a], Jagdeep Singh Sidhu[a], Sacha J. Mooney[b,d], Kathleen M. Brown[a], and Jonathan P. Lynch[a,b,d,1]

[a]Department of Plant Science, Pennsylvania State University, University Park, PA 16802; [b]Division of Agricultural and Environment Sciences, School of Biosciences, University of Nottingham, Leicestershire LE12 5RD, United Kingdom; [c]The James Hutton Institute, Invergowrie DD2 5DA, United Kingdom; and [d]Centre for Plant Integrative Biology, University of Nottingham, Leicestershire LE12 5RD, United Kingdom

Edited by Philip N. Benfey, Duke University, Durham, NC, and approved January 3, 2021 (received for review June 11, 2020)

Mechanical impedance limits soil exploration and resource capture by plant roots. We examine the role of root anatomy in regulating plant adaptation to mechanical impedance and identify a root anatomical phene in maize (*Zea mays*) and wheat (*Triticum aestivum*) associated with penetration of hard soil: Multiseriate cortical sclerenchyma (MCS). We characterize this trait and evaluate the utility of MCS for root penetration in compacted soils. Roots with MCS had a greater cell wall-to-lumen ratio and a distinct UV emission spectrum in outer cortical cells. Genome-wide association mapping revealed that MCS is heritable and genetically controlled. We identified a candidate gene associated with MCS. Across all root classes and nodal positions, maize genotypes with MCS had 13% greater root lignin concentration compared to genotypes without MCS. Genotypes without MCS formed MCS upon exogenous ethylene exposure. Genotypes with MCS had greater lignin concentration and bending strength at the root tip. In controlled environments, MCS in maize and wheat was associated improved root tensile strength and increased penetration ability in compacted soils. Maize genotypes with MCS had root systems with 22% greater depth and 49% greater shoot biomass in compacted soils in the field compared to lines without MCS. Of the lines we assessed, MCS was present in 30 to 50% of modern maize, wheat, and barley cultivars but was absent in teosinte and wild and landrace accessions of wheat and barley. MCS merits investigation as a trait for improving plant performance in maize, wheat, and other grasses under edaphic stress.

root anatomy | soil impedance | phenotype

Soil mechanical impedance is a significant problem that impacts root growth, soil quality, the environment, and crop production on a global scale (1). Soil compaction destroys structure, reduces porosity, limits water infiltration, reduces aeration, and restricts root growth through physical consolidation (2). Compacted soil layers constrain crop productivity by restricting root growth and exploration in deeper soil domains, which in turn limits access to nutrients and water (3). Plants with roots that are able to penetrate hard soil have an advantage in water and nutrient capture at depth, ultimately affording superior performance under drought or low soil fertility (4).

Root phenes [phenes are the fundamental units of a phenotype, in the sense of Lynch (5)] have important roles in plant–soil interactions, nutrient cycling, and soil resource capture (4, 6). Root phenes affect the temporal and spatial distribution of roots in specific soil domains and the ability of roots to obtain mobile and immobile resources (4, 6–9). Mobile nutrients, including nitrate and water, are more available in deeper soil strata due to leaching and evaporation throughout the growth season. In contrast, phosphorus, an immobile soil nutrient, is more available in the topsoil (10). The ability of plants to penetrate through compacted soil is important for capturing mobile nutrients located in deep soil domains.

Root anatomical phenes have a large effect on penetration ability (11). Thicker roots are more resistant to buckling and deflection when encountering hard soils (12, 13). However, in maize, cortical cell wall thickness, cortical cell count, cortical cell wall area, and stele diameter predict root penetration and bend strength better than root diameter (14). Smaller cells in the outer cortical region in maize are associated with increased root penetration of hard layers by stabilizing the root against compression and reducing the risk of buckling and collapse (14). Deeper-rooting maize plants in compacted soils have a reduced cortical cell file number in roots from node three and increased aerenchyma in node four (11). Variation in penetration ability has also been observed among and within species, including cotton (15), maize (16), soybean (16), rice (17, 18), and wheat (19, 20).

In addition to affecting penetration of hard soil, root anatomical phenes also have significant effects on the metabolic costs of soil exploration. In maize (*Zea mays*), the number of cortical cell files and size of cortical cells impacts root respiration, nutrient content, and root elongation into deep soil domains (21, 22). In wheat (*Triticum aestivum*), larger cortical cells are associated with reduced metabolic costs under mechanical impedance (23). Aerenchyma in the root cortex also affects tissue maintenance costs, plant growth, and yield in environments with suboptimal water and nitrogen availability (24–27).

Significance

Multiseriate cortical sclerenchyma (MCS) is a root anatomical phenotype with utility in environments with mechanical impedance. The MCS phenotype is characterized by small cells with thick walls in outer cortical tissue. Genotypes with MCS were associated with greater root lignin concentration, greater tensile strength, and greater root tip bending force compared to non-MCS genotypes. MCS improved root depth and plant growth under mechanical impedance in the greenhouse and field. MCS is heritable and genetically controlled. The identification of anatomical phenes and their genetic control may be an important consideration for breeders for the improvement of crop cultivars with enhanced edaphic stress tolerance.

Author contributions: H.M.S. and J.P.L. designed research; H.M.S., C.F.S., M.T.H., D.J.V., A.C.P., I.B.A., J.S.S., and S.J.M. performed research; H.M.S., C.F.S., M.T.H., D.J.V., A.C.P., I.B.A., J.S.S., S.J.M., K.M.B., and J.P.L. analyzed data; and H.M.S., K.M.B., and J.P.L. wrote the paper.

The authors declare no competing interest.

This article is a PNAS Direct Submission.

[1]To whom correspondence may be addressed. Email: jpl4@psu.edu.

This article contains supporting information online at https://www.pnas.org/lookup/suppl/doi:10.1073/pnas.2012087118/-/DCSupplemental.

Published February 3, 2021.

While relationships of root cortical phenes, like cell size, cell file number, and aerenchyma with root penetration ability have been reported, the functional utility of multiseriate sclerenchyma in outer cortical cells is unknown. Here, we define multiseriate cortical sclerenchyma (MCS) as small lignified cortical cells in the outer cortex of nodal roots. Sclerenchyma are complexes of thick-walled cells, usually lignified, with important mechanical functions. Sclerenchyma tissue enables plant organs to withstand strains from stretching, bending, weight, and pressure while protecting thin-walled cells. Sclerenchyma cells show wide variation in form, structure, origin, and development and frequently have no living protoplasts at maturity (28). However, there are also types of sclerenchyma with living protoplasts and lignified secondary walls, including sclerotic parenchyma (29, 30).

In monocotyledonous plants, peripheral cortical tissues have variable composition. Peripheral cortical tissues may include a complex hypodermis, consisting of one or several layers below the epidermis and centripetally developed internal sclerenchyma layers (31). In response to mechanical injury, cell wall modifications and impregnation by suberin and lignin have been observed in hypodermal and deeper cortical layers (31). Cortical cells that comprise the MCS phenotype are lignified sclerenchyma, a common cell type in plant tissue. However, here we focus on the utility of the spatiotemporal development of MCS, which is distinct from the cell types involved.

Lignin, an umbrella term for a large group of complex aromatic polymers resulting from the oxidative polymerization of hydroxycinnamyl alcohols (32, 33), is associated with mechanical support, water transport in the xylem, and defense against pests and microorganisms in plants (34). In monocots, lignin deposition occurs after the incorporation of hemicellulose and cellulose into the cell wall (35, 36). Lignification begins when cell wall polysaccharides become cross-linked to monolignols through hydroxycinnamic acids (37). Lignin fills the spaces in the cell wall between cellulose, hemicellulose, and pectin to increase the mechanical strength of the cell wall (38). Lignin biosynthesis may be induced by a variety of biotic and abiotic stresses, such as pathogen infection, metabolic stress, wounding, and perturbations in the cell wall structure (39–41). After cellulose, lignin is the second-most abundant organic compound in plants and is predominantly deposited in the walls of secondarily thickened cells, making them rigid and impervious. The extent of lignification depends on the tissue type and function, and supportive tissues typically have greater lignification when compared to parenchyma tissues. Plant lignin content also varies with plant maturity (42, 43), among organs (44–46), among species [e.g., between angiosperms and gymnosperms (47, 48) and between maize and wheat (45, 46, 49)], as well as within species (47).

In roots, lignin concentration is elevated in several tissues, including the endodermis, exodermis (i.e., hypodermis with a Casparian band), and hypodermis (i.e., one or more cell layers adjacent to the epidermis). In maize, the epidermis and endodermis are the outermost and innermost parts the cortex, respectively, while the "central cortex" or mesodermis refers to the region of the cortex between the epidermis and the endodermis. Lignin deposition in the exodermis and the endodermis increases with plant maturity and is marked by cellulosic wall thickenings, often embedded with lignin and sometimes suberin, deposited along the radial, tangential, and transverse walls (50). Lignification of these tissues presumably is induced by a suite of abiotic and biotic factors and modulated by many genes and hormonal pathways. Ethylene, for example, has known roles in lignin deposition (51) in roots and is an important regulator of the development of the Casparian band (52). Genes related to ethylene biosynthesis and signaling are also associated with lignin accumulation in the root (53, 54). In mungbean roots (*Vigna radiata*), lignin content was enhanced by exogenous ethylene exposure and the increased production of lignin was associated with changes in the activity of key lignin biosynthesis enzymes and hydrogen peroxide content (51).

This study is an explicit characterization of the functional utility of the phene we are designating as MCS. In this work, we define the characteristics, development, and regulation of MCS in maize roots and test the utility of this phene for root penetration ability in compacted soils through laboratory, greenhouse, and field experiments.

Results

Characterization of MCS. Thickened, outer cortical sclerenchyma (MCS) cell walls are characterized as living small cells with thick cell walls within the four to seven cell files directly inside the hypodermis (Fig. 1). In genotypes with MCS, thickness of outer cortical cell walls ranged from 7.9 to 11.1 μm, with a mean of 9.5 μm. In genotypes lacking MCS, thickness of outer cortical cell walls ranged from 2.3 to 5.4 μm with a mean of 4.3 μm (*SI Appendix*, Fig. S1). Maize, wheat, and barley lines with MCS were classified as having a cell wall-to-lumen area ratio of greater than 2 and lines without MCS were characterized as having a cell wall-to-lumen area ratio less than 2 (Fig. 1). Thick cell walls present in MCS are primarily thickened with high concentrations of lignin but not pectin or cellulose (Fig. 2). Histological staining of root segments demonstrates that sclerenchyma cells comprising MCS tissue are viable (*SI Appendix*, Fig. S2).

Laser ablation tomography (LAT) can be used to quickly phenotype MCS in cortical cells. Total lignin quantification in plant tissues by traditional chemical methods requires relatively

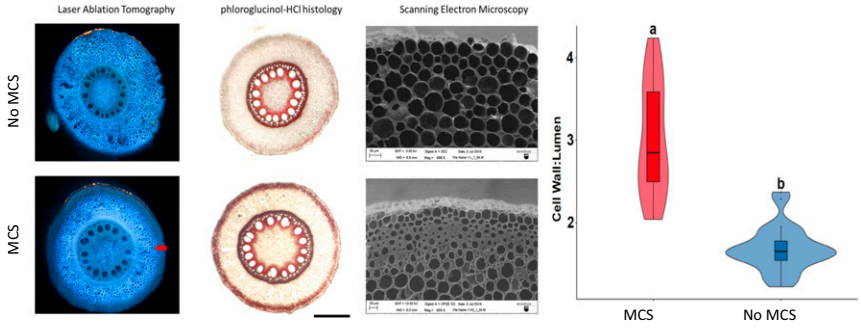

Fig. 1. LAT can be used to quickly and accurately phenotype MCS. Lines with MCS have smaller and thicker outer cortical cells. These thickened cortical cells are stained red with phloroglucinol-HCl due to their high lignin content. Cryo-SEM images show detailed images of the smaller cells with thick cell walls in the outer cortex. (Scale bar, 100 μm.) Violin plot showing median, interquartile range, 95% CIs, and frequency of cell wall:lumen area ratio for MCS ($n = 27$) and non-MCS ($n = 26$) root samples. Letters denote significant differences as determined by Welch's two-sample t-test at a confidence level of $\alpha \leq 0.05$.

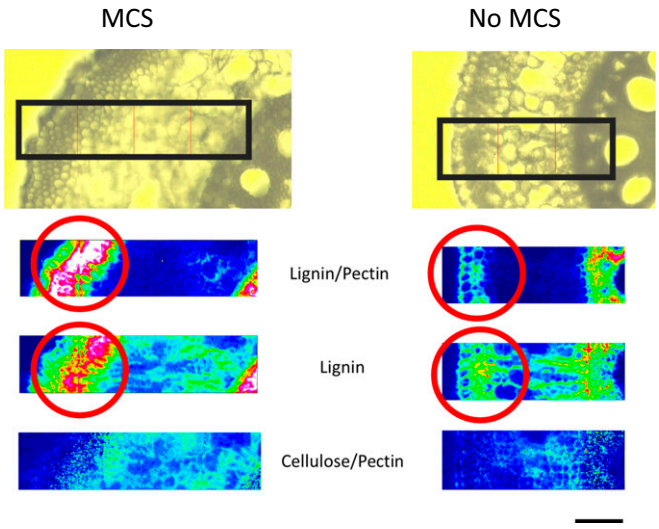

Fig. 2. Fourier-transform infrared spectroscopy demonstrates that outer cortical cells in genotypes with MCS are embedded with lignin (highlighted in red circles) and do not have elevated concentrations of pectin or cellulose when compared to non-MCS genotypes (n = 2). The heatmap displays the concentration of the cell wall component and the hotter the color, the greater the concentration. Images are of nodal, field-grown maize roots. (Scale bar, 50 μm.)

large sample volumes and up to 10-d processing time, while LAT image capture and analysis requires less than 2 min per sample. Roots with MCS had a greater cell wall-to-lumen area ratio in the outer third of the cortex than roots without MCS (Fig. 1). Under UV excitation, cell walls of the outer cortex had a significantly reduced dominant emission spectra in roots with MCS (474.4 nm) compared to roots with no MCS (479.5 nm), as demonstrated through Welch's two-sample t test (Fig. 3). Phenotyping MCS by cell wall-to-lumen area ratio was validated through total lignin quantification assays in the laboratory and histological methods (Figs. 1 and 3). MCS can also be phenotyped qualitatively with phloroglucinol-HCl staining (Fig. 1 and *SI Appendix*, Fig. S3); however, staining methods require significantly more time for sample preparation and imaging compared to LAT. In addition to maize, we observed variation for the MCS phenotype in barley and wheat. LAT of barley and wheat genotypes grown in solution culture demonstrated that these species show genotypic variation for the MCS phenotype (*SI Appendix*, Fig. S4). Genotypes with MCS were classified as having a cell wall-to-lumen area ratio greater than 2 in barley, wheat, and teosinte.

A more detailed analysis of barley (landraces vs. modern cultivars) and wheat (landraces, wild accessions vs. modern cultivars) revealed that the MCS phenotype was only present in modern cultivars, whereas none of the 26 landraces and wild taxa we assessed developed MCS. Furthermore, MCS was observed in ~50% of the modern barley and wheat cultivars. No landraces or wild taxa formed MCS (*SI Appendix*, Figs. S5 and S6 and Table S1). In wheat, MCS was only observed in modern hexaploid varieties and not in diploid wild cultivars and tetraploid landrace and modern varieties (*SI Appendix*, Fig. S5 and Table S1). In addition, MCS was not present at any nodal position in the five *Z. mays* ssp. *parviglumis* accessions studied (*SI Appendix*, Fig. S7 and Table S1).

In greenhouse mesocosms, the MCS phenotype in maize was observed at 25 d after planting at 10 to 12 cm from the root apex in node 2, after the zone of differentiation and lateral root formation (*SI Appendix*, Fig. S8). Cortical cells with MCS did not change their cell wall thickness once it had formed (*SI Appendix*, Fig. S9) or along the root axis (*SI Appendix*, Fig. S8). In the genotypes studied, MCS was not detected in seminal, primary, and first node crown roots or lateral roots (*SI Appendix*, Fig. S10). Its presence was weakly observed in second node crown roots and it became more pronounced in roots emerging from younger nodes with increased diameters. When compared within a nodal position, root diameter was not associated with MCS. However, the proportion of cross-sectional area that was occupied by the stele was significantly positively correlated with MCS (*SI Appendix*, Fig. S11).

Root lignin concentrations were significantly positively correlated with cell wall-to-lumen area ratios (R^2 0.74, $P < 0.05$). No significant differences were observed in root lignin concentrations of primary, seminal, and first node axial roots between genotypes with and without MCS (Fig. 3). Third- and fourth-node crown roots with MCS had significantly greater lignin

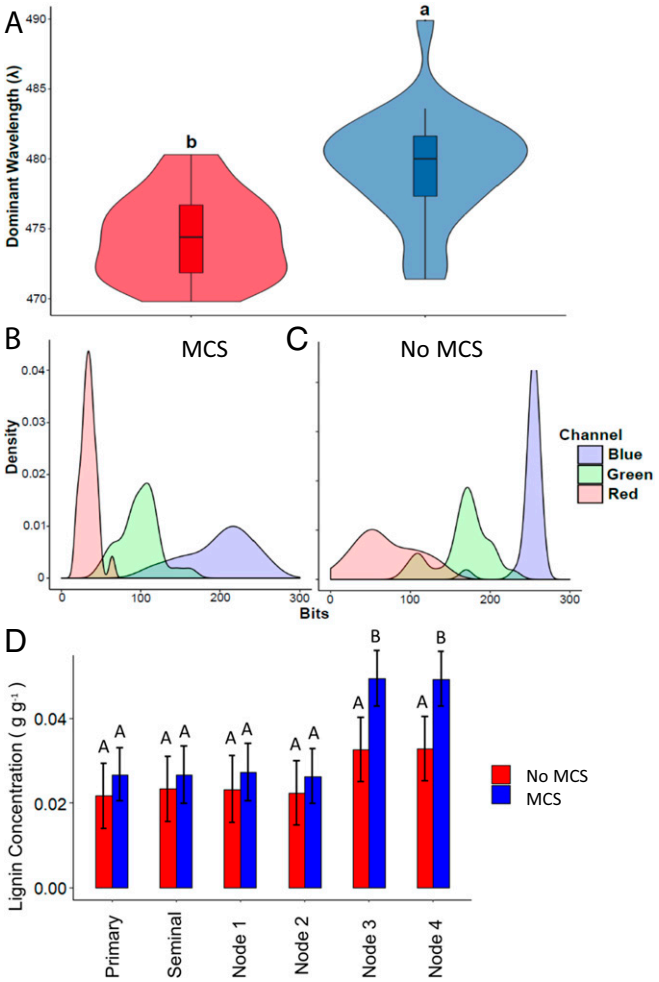

Fig. 3. (*A*) Violin plot showing median, interquartile range, 95% CIs, and frequency of dominant emission wavelength (λ) for the outer cortical region of high (n = 27) and low lignin roots (n = 26). Letters denote significant difference as determined by Welch's two-sample t-test at a confidence level of $\alpha \leq 0.05$. (*B* and *C*) Density plots of modal R, G, and B values for pixels in outer cortical region of roots with MCS (*B*) and non-MCS (*C*). (*D*) Root lignin concentrations and MCS in different root classes and nodes. Root lignin concentrations are not significantly different in primary, seminal, and first- and second-node crown roots in genotypes with and without MCS. Root lignin concentrations were measured in all tissues of the entire root. Roots with MCS had significantly greater lignin concentrations compared to roots with no MCS in third and fourth-node crown roots. Data shown are means ± SE for three genotypes per group (n = 12). Means with the same letters are not significantly different ($P \leq 0.05$).

concentrations compared to roots without MCS. In addition, genotypes with MCS had significantly more lignin in the root tip (0.021 ± 0.004 g g^{-1}) compared to genotypes without MCS (0.01 ± 0.003 g g^{-1}). Total root lignin concentration and the presence of MCS in roots did not correlate with lignin concentrations of stems or leaves (*SI Appendix*, Fig. S12).

MCS development was modulated by ethylene exposure. All non-MCS genotypes formed MCS upon exogenous ethylene exposure (*SI Appendix*, Fig. S13). However, genotypes with MCS did not change the extent of MCS or cell wall thickness upon exogenous ethylene exposure. Ethylene treatment did not influence where MCS began relative to the root apex. No differences in MCS were observed between the ethylene inhibitor, control, and the ethylene and inhibitor treatments. This suggests that ethylene action is not strictly required for MCS, but instead acts as a modulator of MCS initiation (Fig. 4).

Utility of MCS under Mechanical Impedance.

MCS increases tensile and root tip strength. During the tensile test, roots displayed typical elastic–plastic deformation with initially steep force displacement curves in the elastic region before plastic deformation beyond the yield point. In the force displacement curves, two distinct peaks were observed. The first peak marks cortical failure and the second peak marks ultimate tensile failure [see Chimungu et al. (14)]. Tensile breaking force increased with increasing root lignin concentration and cell wall-to-lumen area ratio (Fig. 5 *A* and *C*). Genotypes with MCS were associated with greater cortical tensile strength compared to non-MCS genotypes. In maize, root lignin concentrations were significantly positively correlated with root cortical tensile strength ($R^2 = 0.15$, $P = 0.0034$). In wheat, cell wall-to-lumen area ratios were significantly positively correlated with root cortical tensile strength ($R^2 = 0.29$, $P = 0.0047$). Tensile strength of the root cortex was on average 20% and 28% greater in lines with MCS compared to lines without MCS in maize and wheat, respectively (Fig. 5 *A* and *C*).

Similarly to increased cortical tensile strength, genotypes with MCS had greater root tip strength. In maize roots from nodes 3 and 4, genotypes with MCS had on average 109% greater root tip bending strength (i.e., the force required to bend the root tip) at 3 mm from the root apex compared to genotypes without MCS (Fig. 5*B*). In wheat, genotypes with MCS had on average 57% greater root tip bending strength at 3 mm from the root apex compared to genotypes with no MCS (Fig. 5*D*).

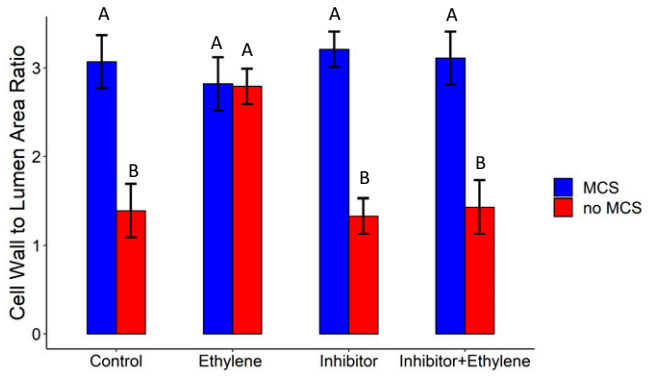

Fig. 4. Ethylene modulates the formation of MCS. Genotypes with no MCS increased their cell wall-to-lumen ratio (a quantitative measure of MCS formation) upon exposure to ethylene. Genotypes with MCS formation did not increase their cell wall-to-lumen area ratio in outer cortical cells upon ethylene exposure. The ethylene inhibitor treatment reversed the ethylene-induced increase in MCS in no MCS genotypes. Data shown are means ± SE for three genotypes per group ($n = 12$). Means with the same letters are not significantly different ($P \leq 0.05$).

MCS increases root penetration of a wax layer. The root penetration ratio through a wax layer ranged from 0.44 to 0.93 across the six maize genotypes studied, where a root penetration value of 1 signifies that all roots penetrated the wax layer and a root penetration value of 0 signifies that no roots were able to penetrate the wax layer. Maize genotypes with MCS had on average 48% greater penetration ability through the hard wax layer compared to genotypes without MCS (Fig. 6 *A* and *B*). Wheat genotypes with MCS had on average 62% greater penetration ability through the hard wax layer compared to genotypes without MCS (Fig. 6 *C* and *D*).

MCS increases root penetration of compacted soil. Compacted greenhouse mesocosms had significantly greater penetrometer resistance at 22- to 45-cm depth compared to mesocosms without compaction (*SI Appendix*, Fig. S14). Upon reaching the compacted zone, roots of the genotypes without MCS increased their cell wall-to-lumen area ratio in the outer cortex by 19% while this ratio remained unchanged in genotypes with MCS. However, in non-MCS genotypes cell wall-to-lumen area ratios did not meet the threshold to be considered MCS (i.e., cell wall-to-lumen area ratio greater than 2) but genotypes with MCS reduced the number of cell files with thickened walls by 45% after the transition from less to more compacted soil (*SI Appendix*, Fig. S14). In addition, MCS was accompanied by larger cells in the mesodermis (i.e., midcortex) (*SI Appendix*, Fig. S14). Interestingly, MCS genotypes had on average 50% greater dry shoot biomass compared to non-MCS genotypes in the compaction treatment while no differences in dry shoot biomass were observed between these genotypes in control conditions (*SI Appendix*, Fig. S14).

Field Experiments. Genotypes with MCS had on average 26% greater D_{75} (the depth above which 75% of the total root length within a core was located) in compacted soil at the Apache Root Biology Center in Willcox, Arizona (ARBC) and on average 18% greater D_{75} in compacted soil at the Russell E. Larson Agricultural Research Center in Rock Springs, Pennsylvania (PSU), compared to lines without MCS (Fig. 7). This indicates that roots with MCS are better able to penetrate hard, compacted soils compared to roots without MCS. Genotypes with MCS had on average 46% and 51% greater dry shoot biomass compared to lines without MCS in compacted soils at the ARBC and PSU, respectively. No significant differences were observed in shoot biomass in the noncompacted treatment between genotypes with and without MCS in either environment (Fig. 7).

Genome-Wide Association Mapping and Quantitative Trait Mapping. MCS is heritable ($H^2 = 0.64$) and genetically controlled. Genome-wide association mapping/studies (GWAS) identified a significant SNP using a Bonferroni-corrected genome-wide threshold value of $-\log(p) = 7.07$. Candidate genes were selected from gene models containing SNPs above the Bonferroni significance threshold. The significant SNP was located in gene model Zm00008a033967 on chromosome 9 and was associated with a MEI2-like RNA binding protein (Fig. 8). This significant SNP on chromosome 9 identified through GWAS overlaps with the 1.5 LOD confidence interval (CI) with a quantitative trait locus (QTL) identified in the IBM population (*SI Appendix*, Fig. S15).

Discussion

We present MCS, a root anatomical phenotype in maize and other cereals and provide evidence for its physiological implications. We evaluated genotypes with and without MCS in different environments, including the growth chamber, greenhouse, and two field sites in order to assess the physiological utility of this phene under mechanical impedance. We demonstrated that MCS can be accurately and rapidly phenotyped using LAT (Figs. 1 and 3) or less rapidly with phloroglucinol-HCl staining (Fig. 1). MCS is characterized by small cells with highly lignified, thick

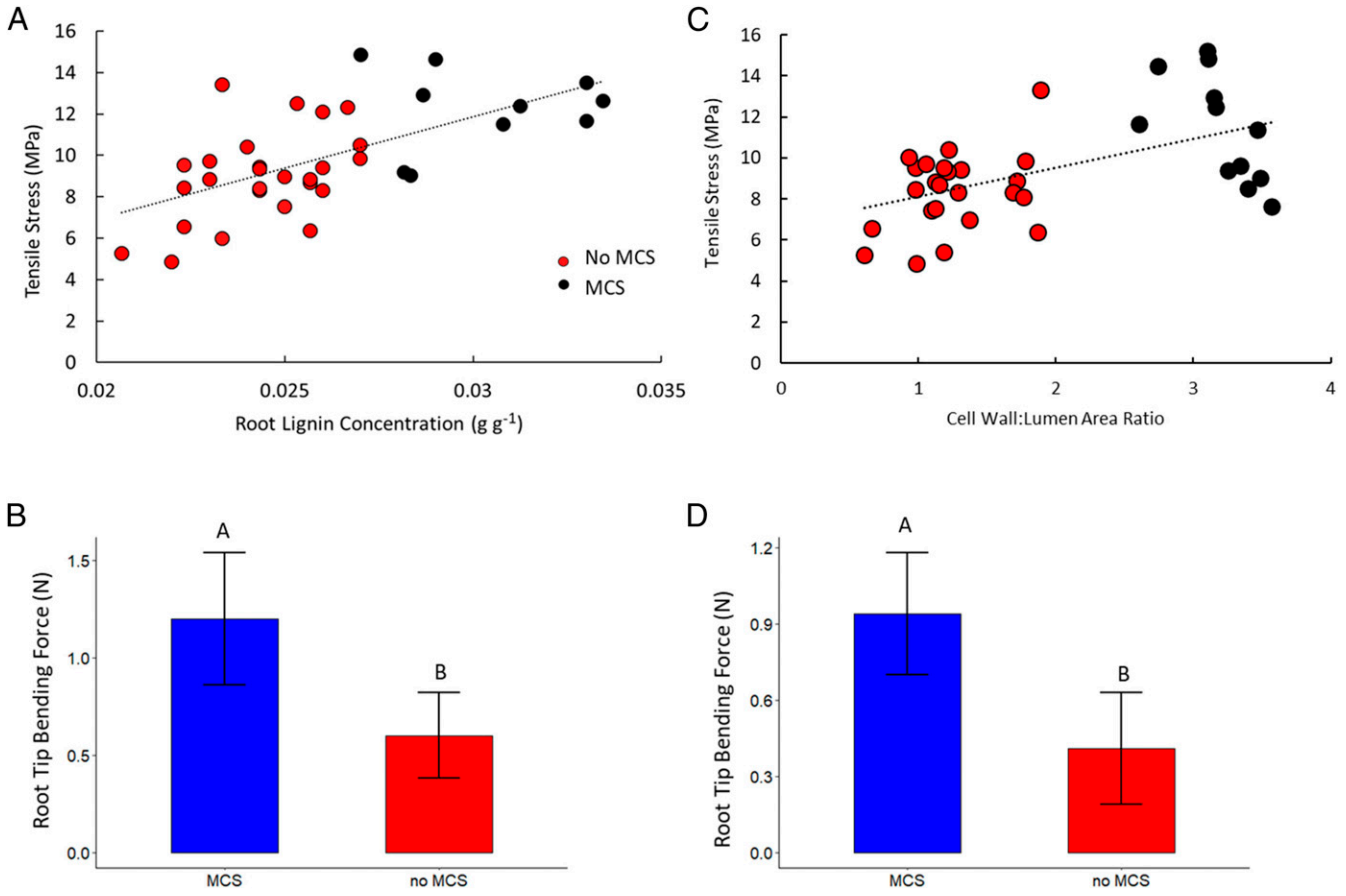

Fig. 5. Root lignin concentration is correlated with tensile stress of the root cortex and root tip bending force. (*A*) Tensile stress of seminal roots, and first-, second-, and third-node crown root in maize is shown at 37 d of growth from greenhouse mesocosms. (*B*) Roots with MCS had a greater root tip bending force compared to tips of roots without MCS in maize. (*C*) Tensile stress of nodal roots in wheat is shown at 30 d of growth from greenhouse mesocosms. (*D*) Tips of roots with MCS had a greater bending force compared to tips of roots without MCS in wheat. Data shown are means ± SE for four replications per genotype from plants grown in greenhouse mesocosms ($n = 12$ in maize, $n = 16$ for wheat with MCS, $n = 32$ for wheat without MCS). Means with the same letters are not significantly different ($P \leq 0.05$) according to Tukey's HSD.

cell walls in the outer cortex (Fig. 2). MCS is modulated by ethylene in genotypes without constitutive MCS (Fig. 4). MCS is associated with enhanced cortical tensile strength and bending force of the root tip (Fig. 5). In the greenhouse and growth chamber, genotypes with MCS were associated with increased penetration of hard soils (Fig. 6). In the field, genotypes with MCS had greater root depth distribution (D_{75}) and greater shoot biomass in compacted soil compared to non-MCS genotypes (Fig. 7).

Cortical cells that comprise the MCS phenotype are lignified sclerenchyma, a common cell type in plant tissue. Sclerenchyma cells can be found in many plant tissues, including xylem, phloem, leaves, fruits, periderm, cortex, and the pith. In roots, sclerenchyma is common in monocotyledons, but rare in dicotyledons and usually presents as a cylindrical arrangement of several cortical cell files either directly beneath the epidermis or next to the endodermis (28). Several species develop subexodermal layers modified with lignin or suberin (but not Casparian bands or suberin lamellae). These lignified subexodermal layers may provide structural support and occur in many species, including *Pontederia*, *Nelumbo* (55), and *Phragmites* (56). While these species have a similar pattern of sclerenchyma when compared to MCS, MCS is characterized by many more lignified cell layers, with thicker cell walls and a distinct temporal development in specific root classes. The term "MCS" refers to the spatial and temporal development of sclerenchyma cells in the root cortex, as described here.

In the present study, LAT and subsequent semiautomatic analysis of images using MIPAR software (57) enabled the rapid quantitative evaluation of MCS, expressed as cell wall-to-lumen area ratios. Strock et al. (58) used the autofluorescent signature of cell walls under UV excitation (355 nm), converted into RGB spectra values, and calculated the dominant emission wavelength within the visible spectrum to detect root colonization by edaphic organisms. With minor adjustments, these methods were adapted in to rapidly identify MCS based on spectral emission of outer cortical cells. Total lignin quantification in plant tissues using traditional chemical analysis requires relatively large sample volumes and up to 10-d processing time (59). We demonstrate that quantitative phenotyping the cell wall-to-lumen area ratio, or spectral analysis by LAT or qualitative phenotyping by phloroglucinol HCl staining, are viable and rapid methods to phenotype MCS.

Thickened cell walls were weakly present in a few second-node crown roots and became more pronounced in younger nodes with increased root diameters (*SI Appendix*, Fig. S10). When compared within node, root diameter was not associated with MCS. However, the proportion of cross-sectional area that was occupied by the stele was positively correlated with MCS (*SI Appendix*, Fig. S11).

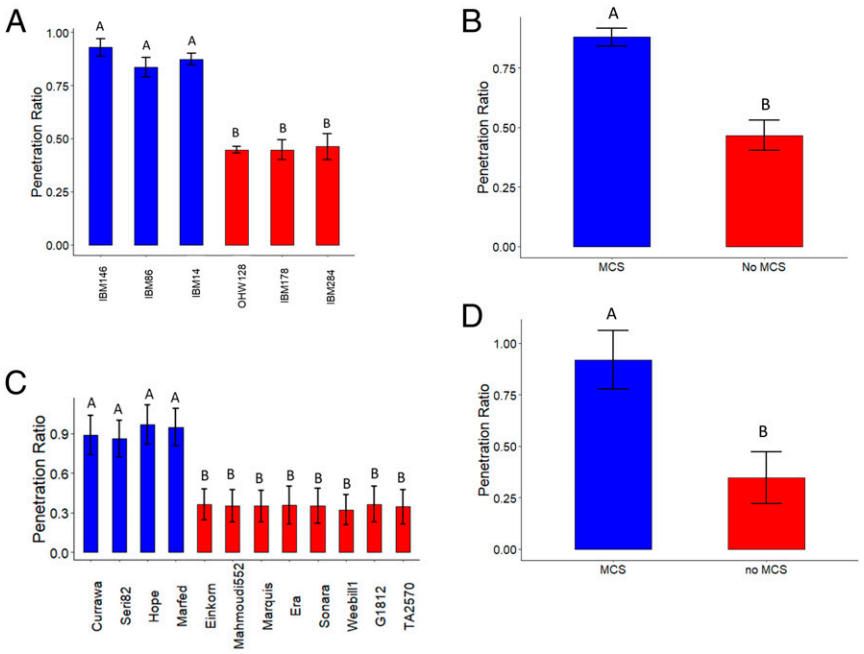

Fig. 6. MCS enables roots to better penetrate soils with a hard wax layer in maize and wheat. (*A*) Maize genotypes with MCS have a greater penetration ratio compared to genotypes with no MCS. (*B*) Average penetration ratio of maize genotypes with MCS compared to the average penetration ratio of non-MCS genotypes. (*C*) Wheat genotypes with MCS have a greater penetration ratio compared to genotypes with no MCS. (*D*) Average penetration ratio of wheat genotypes with MCS compared to the average penetration ratio of non-MCS genotypes. Penetration ratio was calculated as the ratio of the number of roots penetrating the compacted layer to number of roots reaching the compacted layer. Data shown are means ± SE for four replications per genotypes (n = 12 in maize, n = 16 for wheat with MCS, n = 32 for wheat without MCS) of all axial roots. Means with the same letters are not significantly different ($P \leq 0.05$) according to Tukey's HSD.

Our results are consistent with previous reports suggesting that lignification and thickening of cortical cell walls may have utility under edaphic (i.e., soil-related) stress (31, 60, 61). In grasses, hypodermal (and subhypodermal) layers are frequently comprised of small cells with thick walls (31). Lux et al. (31) reported a "multilayered sclerenchymatous hypodermis" in sorghum and

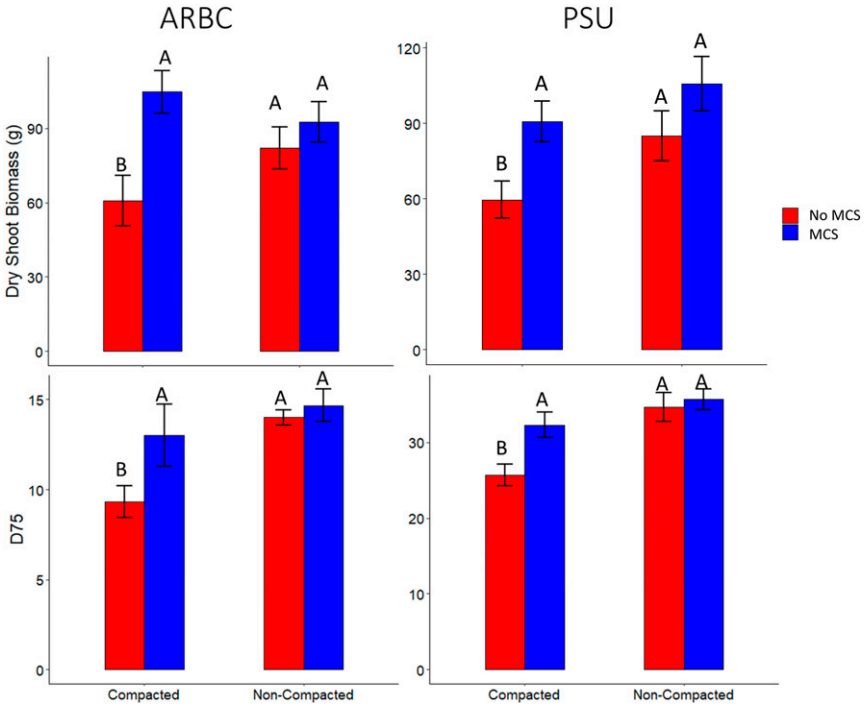

Fig. 7. In the field, genotypes with MCS have significantly greater rooting depth and shoot biomass in compacted soil compared to genotypes without MCS at PSU and ARBC. Data shown are means ± SE for four replications per genotype (n = 12). Means with the same letters are not significantly different ($P \leq 0.05$).

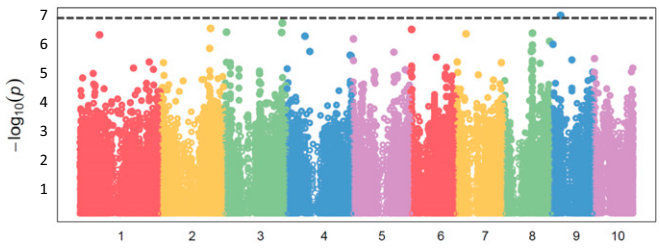

Fig. 8. GWAS identified a significant SNP associated with MCS on chromosome 9. Significant SNPs were identified based on a genome-wide corrected Bonferroni threshold of $-\log(p) = 7.07$.

wheat characterized by small cortical cells with thick walls and speculated that small, thick cells may provide mechanical protection to the root surface and may be an important barrier for inner tissues. In sorghum, a drought-tolerant genotype increased "subhypodermal sclerenchyma with thickened walls" in the stem and to some degree in the roots compared to a drought-susceptible genotype (60). In aerial brace roots in maize, the outer cortex was observed to have heavily lignified secondary walls (62). Thick cell walls of the multiseriate epidermal layer in graminaceous and cyperaceous species increased root resistance to compression (61). However, these studies are largely observational and speculative and do not test the utility of MCS for edaphic stress tolerance. Analysis of numerous root anatomical phenes in maize lines found a correlation of outer cortical cell size with root penetration of a hard wax layer, but did not include further characterization of cells in the outer cortex, or experimental isolation of this phene from other anatomical phenes reported (14). In light of the results presented here, we propose that the small diameter outer cortical cells reported by Chimungu et al. (14) were MCS. The lack of consistent terminology to describe the MCS phenotype further complicates the investigation of this phene. This emphasizes the need for the use of a reference naming system (ontologies) for roots and root phenes (63).

Not all genotypes develop MCS constitutively, but MCS could be induced through ethylene exposure in all genotypes studied. Although MCS was induced by ethylene, 1-MCP, an ethylene inhibitor, did not affect MCS in the absence of ethylene. This suggests that ethylene action is not strictly required for MCS but instead may act as a modulator of MCS initiation: That is, MCS is not regulated by basal endogenous production of ethylene, however, increases in ethylene induce MCS when it is not already present. Levels of 1-MCP used in this study have been shown to be effective in inhibiting root cortical senescence in barley (64) and root cortical aerenchyma in maize (65).

Ethylene has known roles in lignification. Lignification induced by ethylene has implications in mitigating pathogen infection, metabolic stress, wounding, and perturbations in the cell wall structure (39, 40). Ethylene-related genes have been shown to be up-regulated in root tissue in response to root-knot nematode infestation in rice (66) and *Arabidopsis* (53) and are associated with lignin accumulation in the root. MCS and increased lignification of outer cortical cells may also play a role in defense against pests and pathogens.

Genotypes that had roots with high lignin concentrations did not have elevated lignin concentrations in the shoot (*SI Appendix*, Fig. S12). Therefore, MCS cannot be predicted by lignin concentrations in the stem or leaves. Roots of wheat and maize have higher lignin concentrations than stems and leaves (*SI Appendix*, Fig. S12) (44–46). In addition, MCS or elevated root lignin concentration was not consistently present until the emergence of third-node crown roots in maize and nodal roots in wheat, so phenotyping roots at earlier growth stages cannot predict this phenotype. A recent study reported that root cortical phenes in the first and second nodes are not representative of those in subsequent nodes (67). Root lignin content varies among plant organs and generally increases with plant maturity (44).

Root tensile strength, or the maximum force per unit root area required to cause the material to break, plays a role in soil reinforcement and slope stabilization (68) and penetration of hard soils (14). In the present study, root lignin concentrations had a significant, positive relationship with root cortical tensile strength. MCS was more prevalent in roots of younger nodes with greater root diameters. However, MCS was present in wheat and barley lines of thinner diameters, indicating that the development of MCS is not size-related. Previous studies in tree species have demonstrated that as root diameter increased, cellulose, and α-cellulose concentration increased, but the lignin concentration decreased (68, 69). In Chinese pine (*Pinus tabulaeformis*), root tensile strength decreased with increasing root diameter (with roots that had a similar diameter to the present study) in a power function relationship. However, root lignin content had a positive relationship with tensile strength (68). Cellulose content may also play a significant role in increasing tensile strength of the root (70). However, in the present study we did not observe elevated concentrations of cellulose or pectin in MCS (Fig. 2). MCS and increased root lignin concentrations may enable roots with larger diameters maintain tensile strength. Presumably, many factors, including root anatomy and cell wall composition, influence root cortical tensile strength. MCS (and root lignin concentration) plays a significant role in root tensile strength and has utility in penetrating hard soils.

Recent studies have demonstrated that smaller cells in the outer cortical region are associated with increased root penetration in compacted soils. It was proposed that smaller cells in outer cortical cell files stabilize the root against compression and thus reduce the risk of local buckling and collapse during penetration of hard soils (14). Similarly, Striker et al. (61) identified a "multiseriate ring of cells" in graminaceous and cyperaceous species that improved the mechanical strength of the root, even with the presence of aerenchyma in inner cortical cell files. Formation of root cortical aerenchyma significantly weakened root structure in two dicotyledonous species, but the presence of small cells with thick walls in the outer cortex allowed the roots of two monocotyledonous species to maintain mechanical strength, even in the presence of aerenchyma (61, 71). Here we confirm that small cells with thick cell walls in the outer cortical region are important for the ability of maize roots to penetrate hard soils.

Root tensile strength in terms of cortical and stele failure have very different implications. In this study, MCS was positively correlated with the tensile strength of cortical tissue, which is often much weaker than stele tissue (14). Cortical failure, or damage to the cortex due to tensile forces, would have implications in radial water and nutrient update and defense against pathogens if the cortex becomes disrupted. However, if the stele remains intact, the root would be able to perform hydraulic functions and continue to transport water axially. Presumably, if the stele and the growing root tip remain undamaged, regardless of cortical failure, the root would be able to continue growth (72). In addition, the proportion of cross-sectional area that was occupied by the stele was positively correlated with MCS (*SI Appendix*, Fig. S11), which may have synergistic interactions on the tensile strength of the stele.

Metabolic costs of root systems are substantial, and several root anatomical phenes have been demonstrated to improve plant performance in edaphic stress by reducing the nutrient and carbon cost of tissue construction and maintenance (4, 6, 73). Root thickening, which may increase the metabolic cost of the root, in response to mechanical impedance, varies by genotype, and the degree of root thickening is not associated with rooting depth in compacted soils (11). However, root anatomical phenes,

including reduced cortical cell file number, greater cell size in the mesodermis, and increased root cortical aerenchyma, enabled deeper rooting in compacted soil (11). For example, greater cortical cell size or fewer cortical cell files reduce root respiration and nutrient content per unit root length and subsequently improve soil exploration of deep soil domains, water acquisition, and plant performance, and yield in drought environments (21–23). We propose that roots with the smaller, thick outer cortical cells characteristic of MCS combined with fewer cell files with a larger cortical cell size in the mesodermis would improve soil penetration ability and reduce root metabolic costs.

In general, MCS developed ~10 cm behind the root apex and was not observed at the root tip. However, MCS-forming genotypes had greater lignin concentrations and greater resistance to bending at the root tip compared to non-MCS genotypes. Greater lignin concentrations and resistance to root bending at the root tip in genotypes with MCS may enable the penetration of hard soils to obtain mobile soil resources in deep soil domains. We speculate that the development of MCS after the zone of differentiation and lateral root formation occurs so that the thickened outer cortical cells do not impede lateral root emergence through the cortex. MCS was weakly present in second-node crown roots and more apparent in third node and younger root nodes (*SI Appendix*, Fig. S10). MCS may have greater utility in younger nodes due to the typical onset of some types of edaphic stress (e.g., drought and nitrogen limitation) later in plant development. Since root tensile strength generally decreases with root diameter (68), the development of MCS may act to maintain strength of larger diameter roots.

Genetic variation for MCS was found in each of the cereals examined, and heritability was relatively high, suggesting that this phene could be successfully selected in breeding programs using either phenotypic or marker-assisted selection. In a genome-wide association analysis of maize, a significant SNP for MCS was associated with a MEI2-like RNA binding protein. QTL analysis of MCS in a recombinant inbred population produced a very significant peak in the same genomic region. Mei2-like genes are associated with morphogenesis in plants and required in early formation of the basic plant body (74). Zm00008a033967 is root-expressed and its expression is elevated in younger nodes and cortical cells (75). Confirmation of the role of this candidate and identification of additional genes that control MCS will provide molecular tools for breeders to develop genotypes with enhanced edaphic stress tolerance.

MCS exhibited intraspecific variation in three Poaceae species: maize, barley, and wheat (*SI Appendix*, Figs. S1 and S3–S5). However, we did not detect MCS in rice. Rice may have a fundamentally different growth strategy than maize, barley, and wheat (76, 77). In contrast to maize, barley, and wheat, rice develops a suberized and lignified exodermis, which may serve the same role as MCS in terms of pathogen defense and providing mechanical support for the penetration of hard soils. The growth of rice in flooded paddy soils may also alter the fitness landscape of root phenotypes enabling penetration of hard soil.

In addition to compaction tolerance, MCS may also have utility in drought environments. Lignin has important implications in water transport in xylem vessels and radial water transport and uptake through apoplastic barriers, including the endodermis and exodermis (34). Both the exodermis and the endodermis show increased lignin deposition with plant maturity (50). Increased lignification in the endodermis is associated with decreased radial hydraulic conductivity (78). Increased lignification of cortical cells may also reduce root radial hydraulic conductivity. In addition to reduced hydraulic conductivity, MCS may improve plant performance under drought by improving the mechanical strength of the root to promote penetration of hard, dry soils (79). Phenes that enable roots to penetrate hard, compacted soil to capture deep water and nutrients are important targets for crop improvement (4).

Of the taxa we assessed, MCS was observed in modern maize, barley, and wheat accessions. However, we did not observe MCS in wild taxa and landraces of barley and wheat or *Z. mays parviglumis* accessions. Modern agricultural practices have caused significant changes in the soil environment that contribute to increased soil hardness, including a reduction in soil organic matter content and increased soil erodibility (80). In addition, the use of tractors and heavy machinery in modern agricultural practices have substantially contributed to soil compaction (81, 82). Cultivated agricultural soils have a greater bulk density, especially in the topsoil, when compared to native prairie soils (83, 84). It is possible that MCS has been inadvertently selected for in modern breeding programs as a result of evaluation of germplasm in soil subject to these practices.

MCS may promote increased carbon sequestration in deep soil domains. Tissue composition influences the rate and extent of residue decomposition. Recalcitrant carbon compounds, particularly lignin, increase carbon sequestration because they have a long residence time in soil due to the specificity of lignin-degrading enzymes (85). The placement of roots in deeper soil domains may improve carbon sequestration due to decreased microbial activity associated with reduced soil temperatures, less physical disturbance (e.g., tillage), and hypoxia.

We suggest that MCS could be an important trait for edaphic stress tolerance in cereal crops. Genotypes with MCS had greater penetration of hard soils and therefore may enable the capture of deep soil resources. MCS may also increase C sequestration by increasing rooting depth as well as root lignin content. Additional research is necessary in order to assess potential benefits and trade-offs of MCS for plant productivity. Although this work is focused on maize and wheat, we also observed MCS in barley and speculate that the utility of MCS in maize is analogous to other members of the Poaceae. We propose that MCS merits consideration as a trait for plant adaptation to edaphic stress.

Materials and Methods

Plant Material. Six maize genotypes contrasting in root lignin content, which were categorized in preliminary experiments, were grown to assess root penetration ability. Seeds for lines with MCS (small lignified cortical cells) (IBM14, IBM86, IBM146) and non-MCS lines (OHW128, IBM178, IBM284) were provided by Shawn Kaeppler, University of Wisconsin, Madison, WI. The six recombinant inbred lines from two populations designated IBM and OHW were used in all maize experiments (unless otherwise specified) and are described in Burton et al. (86).

Twenty-two genotypes of wheat and its relatives corresponding to different ploidy levels were used in this greenhouse experiment. This includes 4 diploids (*Triticum monococcum*, *Triticum uratu*, *Aegilops taushii*, *Aegilops speltoides*), 6 tetraploids [*Triticum turgidum*, *Triticum timopheevi* (*zhuk.*)], and 12 hexaploids (*T. aestivum*) varieties. The genotypes were procured from the United States National Plant Germplasm System (https://www.ars-grin.gov/npgs/) and their details are listed in the *SI Appendix*, Table S1.

Evaluation of Root Penetration Ability.

Growth chamber. Four replications of each maize and wheat genotype were grown in mesocosms in a temperature-controlled growth chamber (Environmental Growth Chambers, Model GC-36) using a thin wax-layer system (14, 87). Mesocosms were constructed of two stacked polyvinyl chloride cylinders (PVC) pipes, each 13-cm long with an internal diameter of 12.5 cm. A wax–petroleum layer was poured and molded into the bottom of the first layer to simulate a hard-layer. Growth details and experimental set-up are detailed in *SI Appendix*. Plants were grown for 25 d. At harvest, the two parts of the column were separated and the number of roots reaching the wax layer and penetrating the wax layer were counted. The ratio of the number of roots penetrating compared to the number of roots reaching the wax–petroleum layer per plant was expressed as the root penetration index (88). Anatomical samples, 2 cm in length, were collected from all axial roots directly before and after the wax–petroleum layer and preserved in 75% ethanol for anatomical analysis.

Greenhouse mesocosms. The experiments were conducted in a greenhouse at University Park, Pennsylvania. Six maize genotypes (listed above) were planted in a split plot design in two treatments (compacted and noncompacted) with four replications. Plants were grown in individual mesocosms (details in *SI Appendix*). A compaction layer was created with a manual press to an average bulk density of 1.5 g cm^{-3} (details listed in *SI Appendix*). For the noncompaction treatment, mesocosms were filled to a bulk density 1.1 g cm^{-3}.

At harvest (i.e., 40 d after planting), the shoot was removed, the plastic liner was extracted from the mesocosm, cut open, and the roots were washed by rinsing the medium away with low pressure water. Root segments (2 cm in length) of all axial roots at 15 cm below the soil line (~5 cm above the compaction layer) and at 25 cm below the soil line (~10 cm deep within the compaction layer) were collected and preserved in 75% EtOH for anatomical analysis.

Field Experiments. Two field experiments were used to study the utility of MCS in compacted soils. One experiment was conducted at the ARBC the other experiment was conducted at PSU. Six maize genotypes (listed above) were planted in a randomized split plot design in two treatments (compaction and noncompaction). Experimental and environmental details are described in Vanhees et al. (11) and in *SI Appendix*. In the ARBC, the bulk density was 1.6 g cm^{-3} in the compacted treatment compared to 1.48 g cm^{-3} in the noncompacted treatment. In PSU over the 45 cm profile, the bulk density was 1.3 g cm^{-3} in the compaction treatments compared to 1.22 g cm^{-3} in the noncompacted treatments (11). Soils were cored at anthesis (details in *SI Appendix*). At anthesis, two plants per plot were evaluated using the shovelomics method (89). Shoot biomass was collected, and shoot material was dried at 60 °C. Anatomical samples 3 cm in length were collected 3 cm from the crown base from nodes 3 and 4 and stored in 75% ethanol in water (vol/vol).

Evaluation of Root Tensile and Tip Strength and Development of MCS. Six maize genotypes (listed above) were grown in a greenhouse at University Park, Pennsylvania. Plants were grown under the same conditions as listed above for greenhouse mesocosm experiments in four replications per timepoint and plants were harvested at four different time points (15, 20, 25, 30, and 37 d after planting).

At each harvest, roots segments of 6 cm in length were collected 14 to 20 cm from the base of the seminal roots and first-, second-, and third-node crown roots. For harvest time points of 15, 20, 25, 30, and 37 d after planting, roots were preserved in 75% EtOH for anatomical analysis. In addition, at 37 d after planting, a second replication of root segments was collected and refrigerated at 4 °C between moist germination paper to preserve them for up to 24 h until tensile strength testing. Tensile measurements were carried out using a universal testing machine (Instron, model 5866). For tensile strength testing, root samples (55 cm in length) were secured between two grips. The force was recorded with extension at a constant rate of 10 mm min^{-1}. Tensile load was measured using a 100 N load cell (Instron 2525-807 Series) accurate to ±2.5 mN at maximum load. Root tensile strength was calculated as maximum tensile force at cortical failure.

Twelve wheat genotypes (listed above) were grown in four replications in a greenhouse in University Park, Pennsylvania. Growth details are listed in *SI Appendix*. Plants were destructively sampled 35 d after planting by washing the root system with water and collecting root segments from nodal roots, 3 cm in length, ~4 cm from the base of nodal roots, and refrigerated at 4 °C between moist germination paper. Tensile strength was measured with an Instron as described above.

For root tip bending strength, growth details are listed in *SI Appendix*. The root sample was placed on a support and secured with tape 1 cm from the root tip. A pushing probe with a radius of 10 mm was lowered until contact with the sample. The force applied to the root was continuously registered by a 100 N (±2.5) load cell (Instron 2525-807 Series). During the test, the crosshead was lowered at a rate of 10 mm min^{-1} and force required to bend the tip was recorded. Root diameter at 3 mm from the root apex was measured with a caliper. No significant differences were observed in root diameter at the root tip between nodes or genotypes (*SI Appendix*, Fig. S16).

Cryoscanning Electron Microscopy. The cryoscanning electron microscopy (cryo-SEM) technique was used to generate images on the Zeiss Sigma VP-FESEM at the Pennsylvania State University Huck Institutes of the Life Sciences Microscopy Core Facility. Samples of roots with and without MCS were collected at 37 d after planting (greenhouse mesocosm experiment, August 2019). Segments of third-node axial roots 10 to 14 cm from the base of the plant were collected from a genotype with MCS (IBM14) and a genotype without MCS (IBM17) and preserved in 75% EtOH. The sample was mounted on a sample holder and plunged into liquid nitrogen. The sample holder is withdrawn under a vacuum into the cryopreparation chamber where the sample is maintained at a low temperature. The sample was then transferred to the SEM chamber onto a cold-stage module. Variable pressure without sputter coating was used. Voltage was 10 kV and samples were imaged at a temperature of −195 °C.

Fourier Transform Infrared Spectroscopy. Cell wall composition (i.e., cellulose, lignin, pectin) in the outer cortex and mesodermis in genotypes with and without MCS was measured using a Fourier transform infrared spectrometer in two replications. LAT (details below) was used to prepare root-cross sections 5 μm in width of a genotype with MCS (IBM14) and a genotype with no MCS (IBM178). In order to obtain the highest-quality representative spectra of each sample, the measurements were performed on a Bruker Hyperion 3000 Fourier Transform Infrared-Microscope equipped with a 64 × 64 focal plane array detector. Each element on such an array represents an independent infrared sensor. Imaging and data processing details are listed in *SI Appendix*.

Lignin Concentrations through Acid Digestion. Lignin determination was performed according to Goering and Van Soest (90) using the acid-detergent fiber procedures and lignin separation using the permanganate acid-detergent procedure with some minor modifications. Lignin concentrations were determined for whole stems, leaves, and first-, second-, third-, and fourth-node crown roots from each genotype in four replications. In addition, root tips (apical 2 cm) from all root classes were bulked for MCS and non-MCS genotypes for lignin analysis. Plant tissue was collected from a greenhouse mesocosm experiment (37 d after planting, August 2019 experiment), dried, and ground for analysis at Cumberland Valley Analytical Services.

Histology. To confirm spatial accumulation of lignin, phloroglucinol-HCl (Wiesner) staining was used. A 3% phloroglucinol solution in ethanol (wt/vol) was prepared. Roots were hand-sectioned using a razor blade, submerged in the phloroglucinol stain for 10 min, rinsed with de-ionized water, and then transferred to a microscope slide for imaging (details in *SI Appendix*).

Cell viability of sclerenchyma cells forming MCS was confirmed using Evan's blue and propidium iodide. Evan's blue dye penetrates through ruptured or destabilized membranes to stain nonviable cells blue. Evan's blue stain was prepared by mixing 0.25 g of stain in 100 mL of 0.1 M $CaCl_2$ solution at pH 5.6. Root segments 3 cm in length from 5 to 8 cm from the basal portion of the root were collected from wheat roots and placed in 2 mL of the staining solution and imaged. (details in *SI Appendix*). In addition to imaging, Evan's blue bound in destabilized cell membranes was extracted using 1% SDS buffer and quantified spectrophotometrically (details in *SI Appendix*). Propidium iodide staining was performed on the maize IBM46 genotype at 25 d of growth. Longitudinal sections were imaged using a confocal microscope (details in *SI Appendix*).

Ethylene Experiments. Six maize genotypes were grown in solution culture in three treatments: 1) Root zone air application (control), 2) root zone ethylene application, 3) root zone 1-MCP (1-methylcyclopropene, ethylene inhibitor) application, and 4) combined root zone ethylene and 1-MCP application, all applied continuously beginning at seedling transfer to solution culture (details in *SI Appendix*) and according to Schneider et al. (64). After 30 d of growth, root samples were harvested in four replications per genotype per treatment. Root samples from the primary, seminal, and first-, second-, and third-node crown roots were collected 5 to 7, 10 to 12, 15 to 17, 20 to 22, and 25 to 27 cm from the root apex and preserved in 75% EtOH for anatomical analysis.

GWAS and QTL Mapping. MCS was phenotyped on inbred lines of the Wisconsin Diversity Panel (*SI Appendix*, Table S2). Genotypes were grown at the ARBC in 2015 and 2016. Experimental and sampling details are described in *SI Appendix*, and refs. 90–92. In brief, at anthesis, one representative plant per plot was excavated and a 3-cm segment from 5 to 8 cm from the basal portion of the root was excised from a crown root for ablation using LAT (details below). Root images were analyzed using MIPAR (57) software (details below). Phenotypes were used in a Multiple Loci Linear Mixed (93) implemented in the FarmCPU R package (94). Details are listed in *SI Appendix*.

QTL mapping was performed in the IBM population (B73 × Mo17) (95). Genotypes were grown at the Ukulima Root Biology Center in Alma, Limpopo, South Africa in 2011. Experimental and sampling details are described in *SI Appendix*. Composite interval mapping was used to identify QTL with five marker covariates and a window size of 10 cM in R/qtl (96). The LOD

threshold was determined using 1,000 permutations at a significance threshold of 0.05. Details are listed in *SI Appendix*.

Teosinte Experiments. Seeds seven *Z. mays* ssp. *parviglumis* accessions (Ames 21802, Ames 21803, Ames 21808, Ames 21814, Ames 21830, Ames 21861, and PI 384063) and three *Z. mays* ssp. *mexicana* accessions (Ames 8083, Ames 21857, and PI 566674) were used. In the first experiment, plants were grown for 25 d in greenhouse mesocosms and in the second experiment plants were grown for 40 d in greenhouse mesocosms (growth, harvest, and sampling details in *SI Appendix*).

Wheat Experiments. Eighteen genotypes of wheat and its relatives corresponding to different ploidy levels were used in this study. This includes diploids (*T. monococcum*, *T. uratu*, *A. taushii*, *A. speltoides*), tetraploids (*T. turgidum*), and hexaploids (*T. aestivum*) varieties (details are listed in *SI Appendix*, Table S1). Seeds were germinated and grown in solution culture for 30 d (details in *SI Appendix*). At 30 d after germination, three mature nodal roots were harvested from each plant. Root segments, 4 cm from the tip and the base region, from the each harvested nodal root were preserved using a Leica EM CPD300 critical point dryer (Leica Microsystems).

Barley Experiments. Four barley (*Hordeum vulgare*) genotypes consisting of four landraces (BCC776, HOR4727, Nuerenburg, and Tkn24b) and four modern varieties (Barke, MorexIPK, Arena, and Golf) were grown in solution culture as described in Schneider et al. (97) (details in *SI Appendix*). At 45 d after germination, nodal roots were sampled 20 cm from the apex and preserved in 70% ethanol for anatomical analysis.

Anatomical Phenotyping with LAT. Root samples were imaged cross-sectionally using LAT (58, 98). In brief, a UV pulsed laser beam is used to vaporize the root at the camera focal plane and simultaneously imaged. Imaging of root cross-sections was performed using a Canon T3i camera (Canon) and 5× micro lens (MP-E 65 mm) (99, 100).

To characterize roots with and without MCS formation, cortical anatomy and autofluorescent spectral emission from the outer third of the cortex (based on cortical width) were measured from LAT images and using RootScan2 software (details in *SI Appendix*) (101).

Data were analyzed by linear regression, Pearson correlation coefficients, Welch's Two Sample *t*-test, and Tukey's honest significant difference (HSD) using R 4.0.2 (102).

Data Availability. All data have been deposited in Zenodo (103).

ACKNOWLEDGMENTS. We thank John Cantolina at the Pennsylvania State University Huck Institutes of the Life Sciences Microscopy Core Facility for assistance with cryoscanning electron microscopy imaging, and Hojae Yi for support with root biomechanical properties at the Mechanical Testing Laboratory at Pennsylvania State University. H.M.S., M.T.H., A.C.P., J.S.S., K.M.B., and J.P.L. acknowledge support from US Department of Energy ARPA-E Award DE-AR0000821. C.F.S. and J.P.L. acknowledge support from a grant from Foundation for Food and Agriculture Research/Crops of the Future Collaborative. I.B.A. and J.P.L. acknowledge support from a grant from Foundation for Food and Agriculture Research/Crops in Silico. All Pennsylvania State University authors acknowledge support from the US Department of Agriculture National Institute of Food and Agriculture and Hatch Appropriations Project PEN04732. D.J.V. and S.J.M. were supported by a University of Nottingham studentship grant.

1. J. Lipiec, R. Horn, J. Pietrusiewicz, A. Siczek, Effects of soil compaction on root elongation and anatomy of different cereal plant species. *Soil Tillage Res.* **121**, 74–81 (2012).
2. M. Ishaq, M. Ibrahim, A. Hassan, M. Saeed, R. Lal, Subsoil compaction effects on crops in Punjab, Pakistan: II. Root growth and nutrient uptake of wheat and sorghum. *Soil Tillage Res.* **60**, 153–161 (2001).
3. P. B. Barraclough, A. H. Weir, Effects of a compacted subsoil layer on root and shoot growth, water use and nutrient uptake of winter wheat. *J. Agric. Sci.* **110**, 207–216 (1988).
4. J. P. Lynch, Rightsizing root phenotypes for drought resistance. *J. Exp. Bot.* **69**, 3279–3292 (2018).
5. J. P. Lynch, Root phenes for enhanced soil exploration and phosphorus acquisition: Tools for future crops. *Plant Physiol.* **156**, 1041–1049 (2011).
6. J. P. Lynch, Steep, cheap and deep: An ideotype to optimize water and N acquisition by maize root systems. *Ann. Bot.* **112**, 347–357 (2013).
7. J. P. Lynch, T. Wojciechowski, Opportunities and challenges in the subsoil: Pathways to deeper rooted crops. *J. Exp. Bot.* **66**, 2199–2210 (2015).
8. J. P. Lynch, K. M. Brown, New roots for agriculture: Exploiting the root phenome. *Philos. Trans. R. Soc. Lond. B Biol. Sci.* **367**, 1598–1604 (2012).
9. J. P. Lynch, Root phenotypes for improved nutrient capture: An underexploited opportunity for global agriculture. *New Phytol.* **223**, 548–564 (2019).
10. J. Lynch, K. Brown, Topsoil foraging—An architectural adaptation of plants to low phosphorus availability. *Plant Soil* **237**, 225–237 (2001).
11. D. Vanhees, K. Loades, G. Bengough, S. Mooney, J. Lynch, Root anatomical traits contribute to deeper rooting of maize (*Zea mays* L.) under compacted field conditions. *J. Exp. Bot.* **71**, 4243–4257 (2020).
12. K. Jin *et al.*, How do roots elongate in a structured soil? *J. Exp. Bot.* **64**, 4761–4777 (2013).
13. G. M. Whiteley, J. S. Hewitt, A. R. Dexter, The buckling of plant roots. *Physiol. Plant.* **54**, 333–342 (1982).
14. J. G. Chimungu, K. W. Loades, J. P. Lynch, Root anatomical phenes predict root penetration ability and biomechanical properties in maize (*Zea mays*). *J. Exp. Bot.* **66**, 3151–3162 (2015).
15. P. Taylor, M. J. Kasperbauer, Genotypic variation for root penetration of a soil pan. *J. Sustain. Agric.* **13**, 87–94 (1999).
16. V. Bushamuka, R. Zobel, Differential genotypic and root type penetration of compacted soil layers. *Crop Sci.* **38**, 776–781 (1998).
17. A. H. Price, K. A. Steele, B. J. Moore, P. B. Barraclough, L. J. Clark, A combined RFLP and AFLP linkage map of upland rice (*Oryza sativa* L.) used to identify QTLs for root-penetration ability. *Theor. Appl. Genet.* **100**, 49–56 (2000).
18. H. G. Zheng *et al.*, Quantitative trait loci for root-penetration ability and root thickness in rice: Comparison of genetic backgrounds. *Genome* **43**, 53–61 (2000).
19. T. L. Botwright Acuña, E. Pasuquin, L. J. Wade, Genotypic differences in root penetration ability of wheat through thin wax layers in contrasting water regimes and in the field. *Plant Soil* **301**, 135–149 (2007).
20. K. Kubo *et al.*, Genotypic variation of the ability of root to penetrate hard soil layers among Japanese wheat cultivars. *Plant Prod. Sci.* **9**, 47–55 (2006).
21. J. G. Chimungu, K. M. Brown, J. P. Lynch, Large root cortical cell size improves drought tolerance in maize. *Plant Physiol.* **166**, 2166–2178 (2014).
22. J. G. Chimungu, K. M. Brown, J. P. Lynch, Reduced root cortical cell file number improves drought tolerance in maize. *Plant Physiol.* **166**, 1943–1955 (2014).
23. T. Colombi, A. M. Herrmann, P. Vallenback, T. Keller, Cortical cell diameter is key to energy costs of root growth in wheat. *Plant Physiol.* **180**, 2049–2060 (2019).
24. J. Zhu, K. M. Brown, J. P. Lynch, Root cortical aerenchyma improves the drought tolerance of maize (*Zea mays L.*). *Plant Cell Environ.* **33**, 740–749 (2010).
25. R. E. Jaramillo, E. A. Nord, J. G. Chimungu, K. M. Brown, J. P. Lynch, Root cortical burden influences drought tolerance in maize. *Ann. Bot.* **112**, 429–437 (2013).
26. P. Saengwilai, E. A. Nord, J. G. Chimungu, K. M. Brown, J. P. Lynch, Root cortical aerenchyma enhances nitrogen acquisition from low-nitrogen soils in maize. *Plant Physiol.* **166**, 726–735 (2014).
27. J. G. Chimungu *et al.*, Utility of root cortical aerenchyma under water limited conditions in tropical maize (*Zea mays* L.). *F. Crop Res.* **171**, 86–98 (2015).
28. R. Evert, *Esau's Plant Anatomy: Meristams, Cells, and Tissues of the Plant Body: Their Structure, Function, and Development* (John Wiley & Sons, Inc, ed. 3, 2006).
29. I. Bailey, B. Swamy, The morphology and relationships of Austrobaileya. *J. Arnold Arbor.* **30**, 211–226 (1949).
30. K. L. Alvin, R. J. Murphy, Variation in fibre and parenchyma wall thickness in culms of the bamboo *Sinobambusa tootsik*. *IAWA Bull.* **9**, 353–361 (1988).
31. A. Lux, M. Luxová, J. Abe, S. Morita, Root cortex: Structural and functional variability and responses to environmental stress. *Root Res.* **13**, 117–131 (2010).
32. W. Boerjan, J. Ralph, M. Baucher, Lignin biosynthesis. *Annu. Rev. Plant Biol.* **54**, 519–546 (2003).
33. J. Ralph *et al.*, Lignins: Natural polymers from oxidative coupling of 4-hydroxyphenyl- propanoids. *Phytochem. Rev.* **3**, 29–60 (2004).
34. A. M. Boudet, Lignins and lignification: Selected issues. *Plant Physiol. Biochem.* **38**, 81–96 (2000).
35. J. E. Bidlack, D. R. Buxton, R. M. Shibles, I. C. Anderson, Phenylalanine ammonia lyase as a precursory enzyme of legume stem lignification. *Can. J. Plant Sci.* **75**, 135–140 (1995).
36. T. A. Morrison, D. R. Buxton, Activity of phenylalanine ammonia-lyase, tyrosine ammonia-lyase, and cinnamyl alcohol dehydrogenase in the maize stalk. *Crop Sci.* **33**, 1264–1268 (1993).
37. T. A. Morrison, H. G. Jung, D. R. Buxton, R. D. Hatfield, Cell-wall composition of maize internodes of varying maturity. *Crop Sci.* **38**, 455–460 (1998).
38. J. Janssen, "Designing and building with bamboo" (Tech. Rep. 20, International Network for Bamboo and Rattan, Beijing, China, 2000).
39. A. Caño-Delgado, S. Penfield, C. Smith, M. Catley, M. Bevan, Reduced cellulose synthesis invokes lignification and defense responses in Arabidopsis thaliana. *Plant J.* **34**, 351–362 (2003).
40. M. Tronchet, C. Balagué, T. Kroj, L. Jouanin, D. Roby, Cinnamyl alcohol dehydrogenases-C and D, key enzymes in lignin biosynthesis, play an essential role in disease resistance in Arabidopsis. *Mol. Plant Pathol.* **11**, 83–92 (2010).
41. M. Hazman, K. M. Brown, Progressive drought alters architectural and anatomical traits of rice roots. *Rice (N. Y.)* **11**, 62 (2018).
42. E. W. Crampton, L. A. Maynard, The relation of cellulose and lignin content to the nutritive value of animal feeds. *J. Nutr.* 15, 383–395 (1938).
43. K. Knudsen, Carbohydrate and lignin contents of plant materials used in animal feeding. *Anim. Feed Sci. Technol.* **67**, 319–338 (1997).
44. S. Abiven, A. Heim, M. W. I. Schmidt, Lignin content and chemical characteristics in maize and wheat vary between plant organs and growth stages: Consequences for assessing lignin dynamics in soil. *Plant Soil* **343**, 369–378 (2011).

45. M. F. Dignac *et al*., Carbon-13 natural abundance as a tool to study the dynamics of lignin monomers in soil: An appraisal at the Closeaux experimental field (France). *Geoderma* **128**, 3–17 (2005).
46. A. Heim, M. W. I. Schmidt, Lignin turnover in arable soil and grassland analysed with two different labelling approaches. *Eur. J. Soil Sci.* **58**, 599–608 (2007).
47. R. Whetten, R. Sederoff, Lignin biosynthesis. *Plant Cell* **7**, 1001–1013 (1995).
48. T. Higuchi, Lignin biochemistry: Biosynthesis and biodegredation. *Wood Sci. Technol.* **24**, 26–63 (1990).
49. C. A. Palm, C. N. Gachengo, R. J. Delve, G. Cadisch, K. E. Giller, Organic inputs for soil fertility management in tropical agroecosystems: Application of an organic resource database. *Agric. Ecosyst. Environ.* **83**, 27–42 (2001).
50. C. J. Meyer, C. A. Peterson, "Structure and function of three suberized cell layers: Epidermis, epidermis, and endodermis" in *Plant Roots: The Hidden Half*, A. Eshel, T. Beeckman, Eds. (CRC Press Taylor and Francis Group, ed. 4, 2013), pp. 1–20.
51. W. N. Huang *et al*., Ethylene-induced changes in lignification and cell wall-degrading enzymes in the roots of mungbean (*Vigna radiata)* sprouts. *Plant Physiol. Biochem.* **73**, 412–419 (2013).
52. M. Barberon *et al*., Adaptation of root function by nutrient-induced plasticity of endodermal differentiation. *Cell* **164**, 447–459 (2016).
53. T. Fujimoto, T. Mizukubo, H. Abe, S. Seo, Sclareol induces plant resistance to root-knot nematode partially through ethylene-dependent enhancement of lignin accumulation. *Mol. Plant Microbe Interact.* **28**, 398–407 (2015).
54. M. Rhodes, L. Wolltorton, Changes in phenolic acid and lignin biosynthesis in response to treatment of root tissue of the Swedish Turnip (*Brassica napo-brassica*) with ethylene. *Qual. Plant. Plant Foods Hum. Nutr.* **23**, 145–155 (1973).
55. J. Seago, C. Peterson, L. Kinsley, J. Broderick, Development and structure of the root cortex in *Caltha palustris* L. and *Nymphaea odorata* Ait. *Ann. Bot.* **86**, 631–640 (2000).
56. A. Soukup, O. Votrubová, H. Cizkova, Development of anatomical structure of roots of *Phragmites australis*. *New Phytol.* **153**, 277–287 (2002).
57. J. M. Sosa, D. E. Huber, B. Welk, H. L. Fraser, Development and application of MIPAR: A novel software package for two- and three-dimensional microstructural characterization. *Integr. Mater. Manuf. Innov.* **3**, 10 (2014).
58. C. F. Strock *et al*., Laser ablation tomography for visualization of root colonization by edaphic organisms. *J. Exp. Bot.* **70**, 5327–5342 (2019).
59. W. Barnes, C. Anderson, Acetyl bromide soluble lignin (ABSL) assay for total lignin quantification from plant biomass. *Bio Protoc.* **7**, 1–11 (2017).
60. A. A. Salih *et al*., Rooting, water uptake, and xylem structure adaptation to drought of two sorghum cultivars. *Crop Sci.* **39**, 168–173 (1999).
61. G. G. Striker, P. Insausti, A. A. Grimoldi, A. S. Vega, Trade-off between root porosity and mechanical strength in species with different types of aerenchyma. *Plant Cell Environ.* **30**, 580–589 (2007).
62. D. C. Hoppe, M. E. McCully, C. L. Wenzel, The nodal roots of *Zea*: Their development in relation to structural features of the stem. *Can. J. Bot.* **64**, 2524–2537 (1986).
63. G. Lobet *et al*., Demystifying roots: A need for clarification and extended concepts in root phenotyping. *Plant Sci.* **282**, 11–13 (2019).
64. H. M. Schneider, T. Wojciechowski, J. A. Postma, K. M. Brown, J. P. Lynch, Ethylene modulates root cortical senescence in barley. *Ann. Bot.* **122**, 95–105 (2018).
65. B. Hu, A. Henry, K. M. Brown, J. P. Lynch, Root cortical aerenchyma inhibits radial nutrient transport in maize (*Zea mays*). *Ann. Bot.* **113**, 181–189 (2014).
66. C. Kumari, T. K. Dutta, P. Banakar, U. Rao, Comparing the defence-related gene expression changes upon root-knot nematode attack in susceptible versus resistant cultivars of rice. *Sci. Rep.* **6**, 22846 (2016).
67. J. T. Yang, H. M. Schneider, K. M. Brown, J. P. Lynch, Genotypic variation and nitrogen stress effects on root anatomy in maize are node specific. *J. Exp. Bot.* **70**, 5311–5325 (2019).
68. C. B. Zhang, L. H. Chen, J. Jiang, Why fine tree roots are stronger than thicker roots: The role of cellulose and lignin in relation to slope stability. *Geomorphology* **206**, 196–202 (2014).
69. F. M. Thomas, F. Molitor, W. Werner, Lignin and cellulose concentrations in roots of Douglas fir and European beech of different diameter classes and soil depths. *Trees (Berl.)* **28**, 309–315 (2014).
70. M. Genet *et al*., The influence of cellulose content on tensile strength in tree roots. *Plant Soil* **278**, 1–9 (2005).
71. G. G. Striker, P. Insausti, A. A. Grimoldi, R. J. C. León, Root strength and trampling tolerance in the grass *Paspalum dilatatum* and the dicot *Lotus glaber* in flooded soil. *Funct. Ecol.* **20**, 4–10 (2006).
72. D. Scholefield, D. Hall, Constricted growth of grass roots through rigid pores. *Plant Soil* **85**, 153–162 (1985).
73. J. P. Lynch, Root phenes that reduce the metabolic costs of soil exploration: Opportunities for 21st century agriculture. *Plant Cell Environ.* **38**, 1775–1784 (2015).
74. N. De Guzman, "Molecular genetic analysis of plant Mei2-like genes," PhD dissertation, Massey University, Palmerston North, New Zealand (2002).
75. S. C. Stelpflug *et al*., An expanded maize gene expression atlas based on RNA-sequencing and its use to explore root development. *Plant Genome* **9**, 314–362 (2016).
76. N. N. Kadam, X. Yin, P. S. Bindraban, P. C. Struik, K. S. V. V. Jagadish, Does morphological and anatomical plasticity during the vegetative stage make wheat more tolerant of water deficit stress than rice? *Plant Physiol.* **167**, 1389–1401 (2015).
77. J. P. Lynch, J. G. Chimungu, K. M. Brown, Root anatomical phenes associated with water acquisition from drying soil: Targets for crop improvement. *J. Exp. Bot.* **65**, 6155–6166 (2014).
78. K. Ranathunge *et al*., The composite water and solute transport of barley (*Hordeum vulgare*) roots: Effect of suberized barriers. *Ann. Bot.* **119**, 629–643 (2017).
79. K. Yoshimura, A. Masuda, M. Kuwano, A. Yokota, K. Akashi, Programmed proteome response for drought avoidance/tolerance in the root of a C(3) xerophyte (wild watermelon) under water deficits. *Plant Cell Physiol.* **49**, 226–241 (2008).
80. I. C. Grieve, Human impacts on soil properties and their implications for the sensitivity of soil systems in Scotland. *Catena* **42**, 361–374 (2001).
81. S. A. Materechera, Tillage and tractor traffic effects on soil compaction in horticultural fields used for peri-urban agriculture in a semi-arid environment of the North West Province, South Africa. *Soil Tillage Res.* **103**, 11–15 (2009).
82. K. Y. Chan *et al*., Agronomic consequences of tractor wheel compaction on a clay soil. *Soil Tillage Res.* **89**, 13–21 (2006).
83. M. B. David, G. F. McIsaac, R. G. Darmody, R. A. Omonode, Long-term changes in mollisol organic carbon and nitrogen. *J. Environ. Qual.* **38**, 200–211 (2009).
84. R. Matamala, J. D. Jastrow, R. M. Miller, C. T. Garten, Temporal changes in C and N stocks of restored prairie: Implications for C sequestration strategies. *Ecol. Appl.* **18**, 1470–1488 (2008).
85. G. B. De Deyn, J. H. C. Cornelissen, R. D. Bardgett, Plant functional traits and soil carbon sequestration in contrasting biomes. *Ecol. Lett.* **11**, 516–531 (2008).
86. A. L. Burton *et al*., QTL mapping and phenotypic variation for root architectural traits in maize (*Zea mays* L.). *Theor. Appl. Genet.* **127**, 2293–2311 (2014).
87. L.-X. Yu, J. D. Ray, J. C. O'Toole, H. T. Nguyen, Use of wax-petrolatum layers for screening rice root penetration. *Crop Sci.* **35**, 684–687 (1995).
88. S. A. Materechera, A. M. Alston, J. M. Kirby, A. R. Dexter, Influence of root diameter on the penetration of seminal roots into a compacted subsoil. *Plant Soil* **144**, 297–303 (1992).
89. S. Trachsel, S. M. Kaeppler, K. M. Brown, J. P. Lynch, Shovelomics: High throughput phenotyping of maize (*Zea mays* L.) root architecture in the field. *Plant Soil* **341**, 75–87 (2011).
90. H. Goering, J. Van Soest, *Forage Fiber Analysis*. Handbook number 379 (US Department of Agriculture, US Government Printing Office, Washington, DC, 1970).
91. H. M. Schneider *et al*., Genetic control of root anatomical plasticity in maize. *Plant Genome* **13**, e20003 (2020).
92. H. M. Schneider *et al*., Genetic control of root architectural plasticity in maize. *J. Exp. Bot.* **71**, 3185–3197 (2020).
93. Z. Zhang *et al*., Mixed linear model approach adapted for genome-wide association studies. *Nat. Genet.* **42**, 355–360 (2010).
94. X. Liu, M. Huang, B. Fan, E. S. Buckler, Z. Zhang, Iterative usage of fixed and random effect models for powerful and efficient genome-wide association studies. *PLoS Genet.* **12**, e1005767 (2016).
95. M. Lee *et al*., Expanding the genetic map of maize with the intermated B73 x Mo17 (IBM) population. *Plant Mol. Biol.* **48**, 453–461 (2002).
96. K. W. Broman, H. Wu, S. Sen, G. A. Churchill, R/qtl: QTL mapping in experimental crosses. *Bioinformatics* **19**, 889–890 (2003).
97. H. M. Schneider *et al*., Root cortical senescence decreases root respiration, nutrient content and radial water and nutrient transport in barley. *Plant Cell Environ.* **40**, 1392–1408 (2017).
98. B. Hall, A. Lanba, J. Lynch, Three-dimensional analysis of biological systems via a novel laser ablation technique. *J. Laser Appl.* **31**, 022602 (2019).
99. W. Rasband, ImageJ. https://imagej.nih.gov/ij/. Accessed 17 April 2019.
100. T. Smith, J. Guild, The CIE colormetric standards and their use. *Trans. Opt. Soc.* **33**, 73 (1931).
101. A. L. Burton, M. Williams, J. P. Lynch, K. M. Brown, RootScan: Software for high-throughput analysis of root anatomical traits. *Plant Soil* **357**, 189–203 (2012).
102. R Core Team, R: A Language and Environment for Statistical Computing (Version 3.3.1, R Foundation Statistical Computing, Vienna, Austria, 2018).
103. H. Schneider, Multiseriate cortical sclerenchyma enhance root penetration in compacted soils. *Zenodo*. https://doi.org/10.5281/zenodo.4455953. Deposited 21 January 2021.